ACS APPLIED ENERGY MATERIALS
Cite This: ACS Appl. Energy Mater. XXXX, XXX, XXX−XXX
Article
www.acsaem.org

Highly Stretchable Supercapacitors Enabled by Interwoven CNTs Partially Embedded in PDMS

Runzhi Zhang, Junjun Ding, Chao Liu, and Eui-Hyeok Yang*

Department of Mechanical Engineering, Stevens Institute of Technology, Hoboken, New Jersey 07030, United States

Supporting Information

ABSTRACT: We present flexible and stretchable supercapacitors composed of interwoven carbon nanotubes (CNTs) embedded in polydimethylsiloxane (PDMS) substrates. CNTs are grown using atmospheric-pressure chemical vapor deposition (APCVD) on a Si/SiO_2 substrate and then partially embedded into PDMS. This unique process permits a rapid and facile integration of the interwoven CNT−PDMS structure as a flexible and stretchable supercapacitor electrode with a high level of integrity under various strains. The electrochemical properties of the supercapacitors are measured in 30% KOH solution and with a poly(vinyl alcohol) (PVA)−KOH gel electrolyte (i.e., all-solid-state flexible supercapacitor). The measured capacitance of the supercapacitor is 0.6 mF/cm^2 in 30% KOH solution and is 0.3 mF/cm^2 with a PVA−KOH gel electrolyte at a scan rate of 100 mV/s, showing a consistent performance under stretching from 0% to 200% and bending/twisting angles from 0° to 180°. The stretching test is performed for 200 cycles from 0% to 100%, after which its capacitance is attenuated by 25%. The all-solid-state stretchable supercapacitors show a stable galvanostatic performance during and after 10 000 charge/discharge cycles with its capacitance maintained.

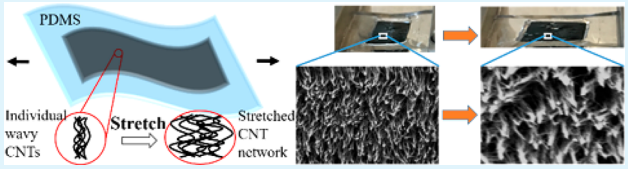

KEYWORDS: *stretchable, supercapacitors, flexible, electronics, vertically aligned carbon nanotubes*

1. INTRODUCTION

Batteries and supercapacitors are both important components in energy storage systems. Unlike batteries, no chemical and phase changes are involved in the charging and discharging in supercapacitors. Therefore, supercapacitors have an almost unlimited cyclability, on the order of 10^5−10^6 times.[1] Sufficiently large accessible electrode areas of the supercapacitors enable high capacitance and high energy density. Supercapacitors have much higher power densities (from 5 to 55 kW/kg) than Li-ion battery (from 0.4 to 3 kW/kg),[2] which makes them ideal for high-power devices, such as regenerative braking and load leveling systems, with great potential to complement batteries or electrolytic capacitors. By making supercapacitors flexible, it opens up applications ranging from self-powered rollable displays to wearable and lightweight electronics.[3−10]

Typically, supercapacitors consist of two electrodes, an electrolyte, and a separator arranged between the two electrodes. Electric energy storage occurs at the electrode/electrolyte interface of both positive and negative electrodes or through surface oxidation/reduction.[11] High surface area, electrical conductivity, mesoporosity, and electrolyte accessibility are important properties desired for an ideal electrode material.[12,13] Carbon in its various forms, such as activated carbon, carbon fibers, carbon clothes, carbon aerogels, graphene, and carbon nanotubes (CNTs), has been widely studied as an electrode material for electrochemical capacitors.[14−33] The capacitance and charge storage/delivery essentially depend on the variation of electrode materials because poor accessibility of the carbon surface to the electrolyte has been confirmed to be the most important reason for the absence of proportionality between specific capacitance and surface area of the materials.[34,35] CNTs are an attractive electrode material toward high performance supercapacitors owing to their high electrical conductivity, high charge transport capability, chemical stability, and an appropriate balance between the surface area and the mesoporosity of a carbon material, which provide easier access for electrolyte ions to form an electrical double layer on the interface between electrode and electrolyte.[36−40] In recent years, vertically aligned carbon nanotubes (VACNTs) have been widely studied for supercapacitor applications,[11,41−48] owing to their advantages of exhibiting a combined charge capacity from all individual tubes, high effective surface area (2200 m^2/g[49]), electrical conductivity (7−14 S/cm[50]), power density (98.9 kW/kg[49]), and energy density (24.7 Wh/kg[49]). Several studies have been conducted to investigate the fabrication and characterization of CNT-based flexible supercapacitors.[51,14,52−55,27,28,56−59] Though significant accomplishments have been demonstrated for flexible/stretchable supercapacitors, fabrication processes are often complicated or time-consuming. Facile fabrication process, along with the ability to accommodate various mechanical disturbances (i.e., large bending, twisting and stretching), would be beneficial for practical applications of flexible and stretchable supercapacitor.

Received: February 2, 2018
Accepted: April 10, 2018
Published: April 10, 2018

DOI: 10.1021/acsaem.8b00156
ACS Appl. Energy Mater. XXXX, XXX, XXX−XXX

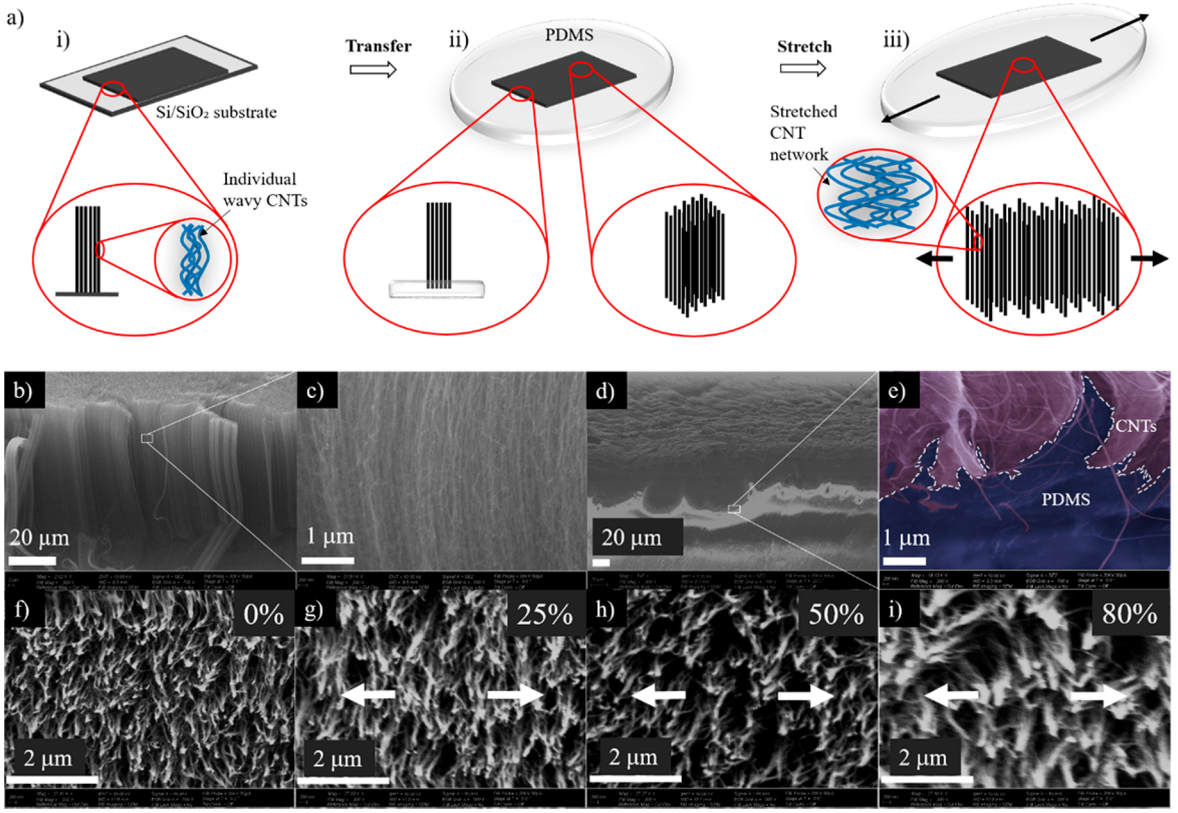

Figure 1. Schematics of the fabrication procedure and illustration of the shape change of interwoven CNTs under stretching of the PDMS substrate. (a) Schematics depicting the fabrication procedure and the stretching of CNT−PDMS structures. (i) Interwoven CNTs are grown on the Si/SiO_2 substrate via APCVD. The CNTs consist of wavy nanotubes and individual nanotubes are mechanically and electrically connected as a CNT network. (ii) Grown CNTs are partially embedded in PDMS. (iii) Individual nanotubes are still interconnected when CNT−PDMS structure is stretched. SEM images of (b, c) cross-sectional view of a CNT carpet grown on the Si/SiO_2 substrate and (d) cross-sectional view of a CNT carpet transferred onto PDMS. The growth and characterization of CNTs have been regularly performed by the author's group and are reported elsewhere.[61,62] (e) Interface area between the CNT carpet and PDMS (white dashed line), showing that the CNT carpet is partially embedded in PDMS, and (f−i) the top views of CNT-PDMS structure under 0%−80% stretching strains.

Here we demonstrate a facile and reliable fabrication of stretchable supercapacitors based on the partial embedding of vertically aligned carbon nanotubes (VACNTs) in PDMS, which enables the stretchable supercapacitors with a high level of integrity under various strains. We grow 100 μm thick interwoven CNTs via atmospheric-pressure chemical vapor deposition (APCVD). We transfer the CNTs from as-grown Si/SiO_2 substrates onto partially cured PDMS to partially embed the CNTs into PDMS, after which the fully cured PDMS strongly holds the CNTs to sustain various strains. We characterize the electrochemical properties and the mechanical flexibility of CNT−PDMS structure in a liquid electrolyte as well as with a gel electrolyte, showing a stable charge/discharge performance under various strain values (stretching, bending, and twisting) for multiple cycles.

2. EXPERIMENTAL SECTION

2.1. Growth of Interwoven CNTs. CNTs were grown via atmospheric-pressure chemical vapor deposition (APCVD). The APCVD setup and the recipe are shown in Figure S1. The substrate of Si/SiO_2 chip, consisting of 5 nm Al and 3 nm Fe as catalyst deposited on the surface, was prepared via physical vapor deposition (PVD). Then the substrate was placed in the tube furnace for APCVD growth. The furnace temperature was increased to 750 °C with 500 sccm Ar flow, and interwoven CNTs were grown at 750 °C for 15 min with 60 sccm H_2 and 100 sccm C_2H_4. After the growth, the CVD tube was rapidly cooled down to room temperature by opening the furnace cover, while maintaining Ar flow. While the grown CNTs were generally vertically aligned, they are composed of individual wavy nanotubes, which are mechanically cross-linked with each other.

2.2. Transfer of CNTs onto PDMS. To fabricate VACNT−PDMS structures with a high level of integrity for stretchable supercapacitor electrodes, we optimized the curing condition of PDMS, whereby the PDMS fully wetted the roots of individual CNT carpets upon the full curing of PDMS and eventually CNTs were partially embedded into PDMS. Since VACNTs consist of wavy nanotubes individually entangled with each other, the entire VACNT carpet retains mechanical and electrical integrity during various levels of stretching, bending, or twisting. First, a liquid mixture of PDMS base and curing agent (Sylgard 184 Silicone Elastomer, Dow Corning) were mixed with a ratio of 10:1 and degassed under reduced pressure in a vacuum pump to remove bubbles. Then, the liquid PDMS was heated on a hot plate at 65 °C for about 30 min. At this stage, PDMS was not fully cured. The CNT carpet was placed face-to-face onto the partially cured PDMS. We let PDMS infiltrate between each individual carbon nanotube, owing to the capillary effect and the viscoelastic property of PDMS. As a result, tips of interwoven CNTs were embedded into PDMS. To fully cure PDMS, the CNT−PDMS sample was left in an ambient condition for 12 h. After PDMS is fully cured, the CNT−PDMS substrate was successfully peeled off from the Si/SiO_2 substrate, owing to the stronger hold of one end of the CNTs embedded in PDMS than the adhesion between CNTs and the Si/SiO_2 substrate.

2.3. Fabrication Process of the All-Solid-State Flexible Supercapacitor. PVA−KOH gel electrolyte was fabricated by mixing 1 g of poly(vinyl alcohol) (PVA) powder with 1 g of KOH powder in

DOI: 10.1021/acsaem.8b00156
ACS Appl. Energy Mater. XXXX, XXX, XXX−XXX

10 mL of DI water and mixed at 60° for around 1 h, while continuously stirring until it took on a homogeneous viscous and clear appearance. PVA−KOH gel electrolyte was dripped onto the surface of the CNT−PDMS structures. Care was taken to ensure one end of the CNT carpet was not wetted in order to function as the electrical contact of the electrode with the conductive wires. Carbon paste was used to ensure a good conductivity of the CNTs and the conductive wires. After dripping PVA−KOH gel electrolyte on the surface of the electrodes, all-solid-state flexible supercapacitors were integrated by stacking two electrodes face-to-face into sandwiched system.

2.4. Electrochemical Measurements and Calculations. The electrochemical performance of CNT−PDMS structures as supercapacitor electrodes was characterized using cyclic voltammetry (CV) in a three-electrode configuration as shown in Figure S3, via potentiostat, whereas the all-solid-state flexible supercapacitor was characterized in a two-electrode configuration. Platinum (Pt) foil was used as a counter electrode and Ag/AgCl (sat. KCl) as a reference electrode. The capacitances of the electrodes were calculated as a capacitance per area (F/cm^2). The average capacitance was normalized per area of the samples and was estimated according to the following equation:[51,30,60]

$$C = \frac{\int_{E_1}^{E_2} I \, dV}{\Delta V \times V \times A}$$

where I is the current, A is the area of the supercapacitor, ΔV is the scanning rate, E_1 and E_2 are the voltage, and $V = E_2 - E_1$.

3. RESULTS AND DISCUSSION

Figure S1 and Figure 1a illustrate schematics of the fabrication procedure and shape-change of interwoven CNTs partially embedded in PDMS substrate, respectively. To fabricate stretchable supercapacitors that work under very large strains, we developed a unique transfer process of partially embedding CNTs in partially cured PDMS. We optimized the curing condition of PDMS, so that the partially cured PDMS became tacky but not wet (e.g., a flat pair of tweezers touching the surface of PDMS when removed would draw a string of PDMS that snaps back without wetting the tweezers). The different states of the PDMS curing process are shown in Figure S2. A scanning electron microscope (SEM) (Auriga Small Dual-Beam FIB-SEM, Carl Zeiss, Jena, Germany) was used to characterize the samples. Figures 1b,c show the 94 μm thick carbon nanotube carpets vertically grown from aluminum (5 nm thick)/iron (3 nm thick) catalyst layers deposited on a Si/SiO$_2$ substrate. Figure 1d shows a successfully transferred CNT carpet onto PDMS. Figure 1e depicts the interface (white dashed line) between a CNT carpet and PDMS, showing that tips of individual nanotubes are embedded in PDMS. Figures 1f−i give SEM images showing the top views of CNTs on PDMS under 0%−80% stretching strains. It should be noted that CNTs, albeit they are generally vertically aligned, consist of wavy nanotubes individually entangled with each other, in which individual nanotubes are mechanically cross-linked. When mechanical strains are applied (i.e., when the device is stretched or twisted), the lateral expansion of the nanotube network retains the entanglement, keeping their mechanical and electrical integrity.

As shown in Figures 1f−i, the spacing between individual CNTs is increased during stretching. The interwoven CNTs are laterally deformed under the lateral elongation of PDMS substrate because the bottom tips of CNTs are clearly embedded into PDMS (Figures 1d,e). We characterized the effect of the PDMS stretching on individual CNTs using Raman spectra. No obvious shift of Raman peak position and intensity ratio (I_D/I_G) shown in Raman spectra suggest that individual CNTs were not under significant strain during the PDMS stretching. The Raman spectra of the CNTs on the Si/SiO$_2$ substrate and the CNT−PDMS structure are shown in Figure 2. The Raman spectra were obtained using Horiba

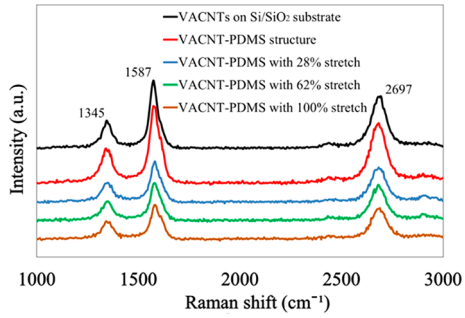

Figure 2. Raman spectra of CNTs on the Si/SiO$_2$ substrate, interwoven CNTs embedded in PDMS without strain applied to the substrate, and CNTs embedded in PDMS under 28%, 62%, and 100% stretching strains. The Raman spectrum of the CNTs on the Si/SiO$_2$ substrate showed a D peak at 1345 cm^{-1}, a G peak at 1587 cm^{-1}, and a 2D peak at 2697 cm^{-1}. No obvious shift of the G peak during and following the substrate stretching indicates that individual nanotubes may not have been subjected to strain during the substrate stretching. The intensity ratio (I_D/I_G) under 0%, 28%, 62%, and 100% stretching were 0.6130, 0.6276, 0.5952, and 0.6293, respectively.

Xplora system with an Andor iDus 420 detector with a 3.5 mW, 532 nm laser. The D peak originates from a hybridized vibrational mode associated with graphene edges, indicating the presence of some disorder to the structure. The more prominent D and 2D peaks compared with the single wall CNTs indicate the multilayer configuration. The G peak is highly sensitive to strain effects in sp^2 nanocarbons and can be used to probe the strain induced by external forces. The intensity ratio of the D and G peaks (I_D/I_G) is widely used to measure the quality with nanotubes as the literature reports that the Raman peak and the intensity ratio of the D and G peaks (I_D/I_G) are very sensitive to the uniaxial strains.[63−67] We measured the Raman peak position and intensity ratio (I_D/I_G) of CNT−PDMS structure under 0%, 28%, 62%, and 100% stretching strains from several different locations. We also performed measurements six times to obtain average values. The Raman spectrum of the CNTs on the Si/SiO$_2$ substrate showed a D peak at 1345 cm^{-1}, a G peak at 1587 cm^{-1}, and a 2D peak at 2697 cm^{-1}. No obvious shift of the G peak was observed when we stretch the CNT−PDMS structure from 0% to 80%, indicating that individual nanotubes were under little strain during substrate stretching. The Raman intensity ratios (I_D/I_G) under 0%, 28%, 62%, and 100% stretching strains were 0.6130, 0.6276, 0.5952, and 0.6293, respectively. There was no obvious change in the intensity ratio I_D/I_G, indicating the interwoven CNTs remains intact after repeated stretching cycles.

Figure 3 and Figure S4 show cyclic voltammetry (CV) of the flexible supercapacitor measured with 30% KOH solution and PVA−KOH gel electrolyte. The flexible supercapacitor demonstrated good electrochemical stability and capacitive behaviors at scan rates from 300 to 1000 mV/s. As shown in Figure S4a, the CV profile of the supercapacitor is very close to a rectangular shape even at a high scan rate; this implies that the CNT−PDMS structure works as a typical electrochemical

DOI: 10.1021/acsaem.8b00156
ACS Appl. Energy Mater. XXXX, XXX, XXX−XXX

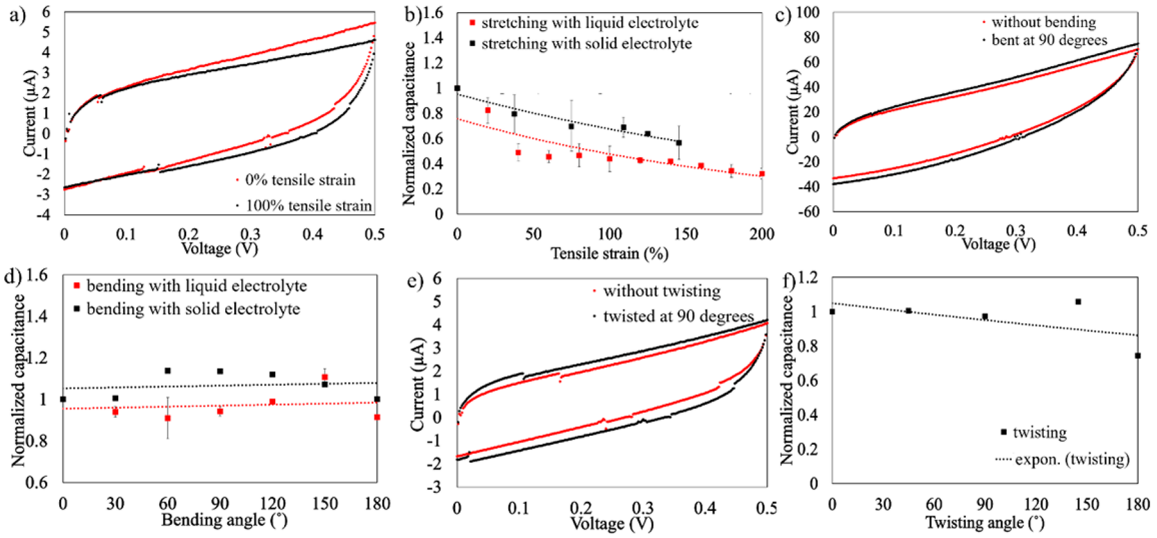

Figure 3. Performance of the supercapacitors measured with PVA−KOH gel electrolyte and with 30% KOH solution. (a) CV curves of the all-solid-state flexible supercapacitors without tensile strain and with 100% tensile strain at the scan rate of 1 V/s. (b) Normalized capacitance of the all-solid-state flexible supercapacitors as a function of tensile strains in comparison with that measured in liquid electrolyte. (c) CV curves of all-solid-state flexible supercapacitors without bending and with 90° bending angle at the scan rate of 1 V/s. (d) Normalized capacitance of the all-solid-state flexible supercapacitors as a function of bending angles in comparison with that measured in liquid electrolyte. (e) CV curves of the all-solid-state flexible supercapacitors without twisting and with 90° twisting angle at the scan rate of 1 V/s. (f) Normalized capacitance of the all-solid-state flexible supercapacitors as a function of twisting angles.

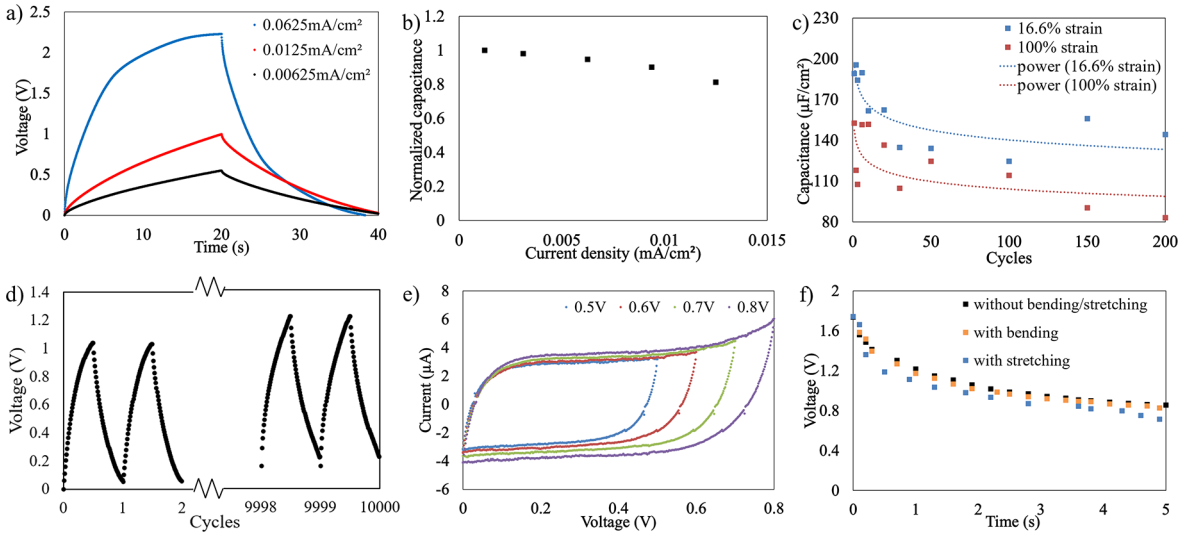

Figure 4. Galvanostatic charge/discharge performance and cyclic behavior. (a) Galvanostatic charge/discharge curves at different current density. (b) Normalized capacitance as a function of discharge current density. (c) Specific capacitance as a function of 200 stretching cycles measured in liquid electrolyte. (d) Cycle life of the all-solid-state flexible supercapacitors at a constant current density of 2.00 mA/cm^2 for 10 000 cycles. (e) CV curves of voltage ranges from 0.5 to 0.8 V. (f) Voltages measured from the diode versus discharge time.

double-layer capacitor electrode and has a relatively small equivalent series resistance.[68] The capacitance decreased with the increased scan rates from 50 to 1000 mV/s (Figure S4b), which is attributed to the increased amount of ions and the increase of the ion transport related resistance.[68] The calculated capacitance of the electrode in KOH solution was 170 and 140 μF/cm^2 with PVA−KOH gel electrolyte at a high scan rate of 1000 mV/s, which were 28% and 47% of the capacitance at the scan rate of 100 mV/s, respectively, comparable to the values reported in the literature (0.21−4.99 mF/cm^2).[52,16,3,69−74] In this experiment, the CNT−PDMS structure was stretched from 0% to 200% and bent from 0° to 180° (bending radius approximately 4 mm) in 30% KOH solution, and the all-solid-state structure was stretched up to 150%, bent up to 180°, and twisted up to 180°. The photographed images of the flexibility measurements are shown in Figure S5. With the increase of strain, the CNT carpet would be deformed while individual nanotubes remain entangled with each other as the spacings between individual nanotubes were increased. Similar deformation would be caused by bending (one side was stretching and the other side was compressing) or twisting (shear stress would deform the shape of CNTs). When larger strains were applied up to the limit of tensile strength of fully cured PDMS, fracture would occur in PDMS. Since two electrodes were used for the all-solid-state flexible supercapacitor, the whole integrated unit fractured if one electrode was broken. This is the reason why

DOI: 10.1021/acsaem.8b00156
ACS Appl. Energy Mater. XXXX, XXX, XXX−XXX

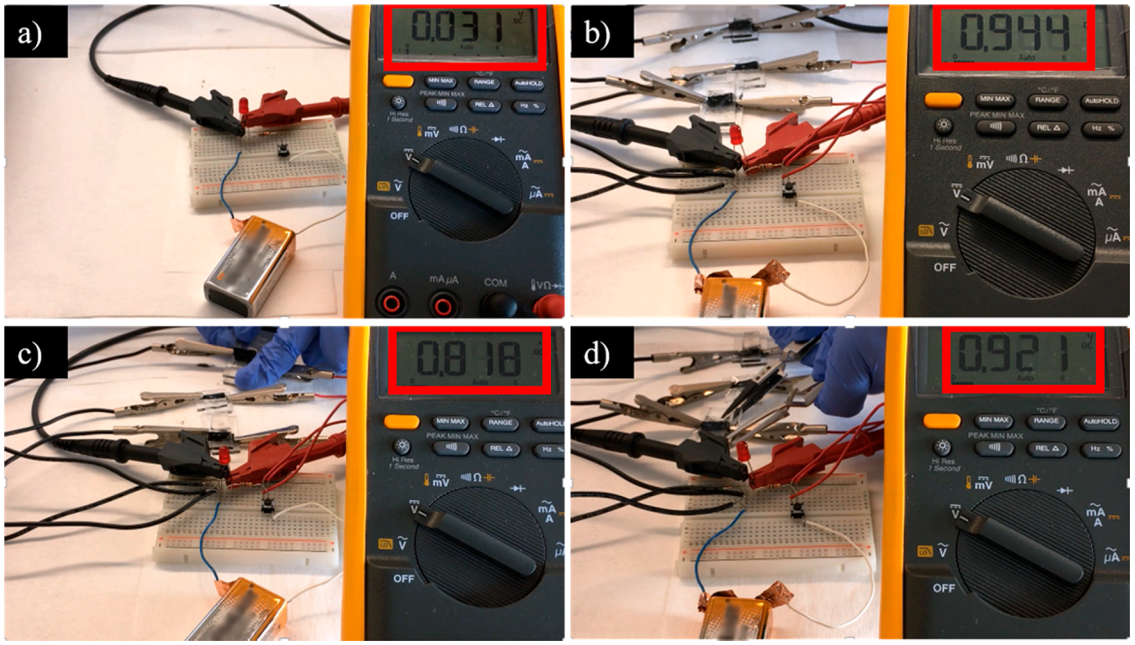

Figure 5. Demonstration of discharge performance of an all-solid-state flexible supercapacitor. (a) Discharge performance without the supercapacitor, showing that the voltage across the diode was instantly dropped from 1.743 to 0.051 V once the battery was disconnected. (b) Discharge performance with the supercapacitor connected to the diode in parallel. The diode voltage was dropped from 1.738 to 0.944 V, after the supercapacitor was discharged for 3 s. (c) Under the supercapacitor stretching (about 50%), the diode voltage was dropped from 1.742 to 0.818 V, which was similar to the discharge performance without stretching. (d) Discharge performance with the supercapacitor under bending. After the supercapacitor was discharged for 3 s, the diode voltage was dropped from 1.743 to 0.921 V, showing the supercapacitor's discharge performance under various mechanical disturbances.

the all-solid-state flexible supercapacitor was measured to be stretched up to 150%, while the one measured in ionic liquid electrolyte was stretched up to 200%, until they show any fatigue. We tested the stretchability of the samples in random directions each time. The results did not show anisotropic electrical properties. Figure 3b shows the average values of the results. Figures 3a, 3c, and 3e show CV curves of the all-solid-state flexible supercapacitor under strain (100% tensile strain), bending (90° bending angle), and twisting (90° twisting angle) states in comparison with the curves without stretching, bending, or twisting. Under these mechanical disturbances, near rectangular CV curves similar to those without disturbances were obtained, indicating a good capacitance behavior of the flexible supercapacitor under strain. Figures 3b,d,f show that this supercapacitor exhibits a good flexibility and stretchability under these mechanical deformations. The capacitance was attenuated by 50% of its value without stretching, when the supercapacitor was stretched by 200%. The capacitance value was consistent at 160 μF/cm^2 at a scan rate of 1000 mV/s under various bending and twisting angles from 0° to 180°.

Galvanostatic charge/discharge performance and cyclic behavior of the supercapacitors are shown in Figure 4. As shown in Figure 4a, galvanostatic charge/discharge curves at small current density show a nearly triangular shape which indicated the good capacitive behavior with a high Coulombic efficiency. With the increase of the current density, the charge and discharge parts in the charge/discharge curves are no longer linear and show an asymmetric capacitance behavior. In Figure 4b, the supercapacitors showed a stable charge/discharge behavior under various discharge current densities. The capacitance of the supercapacitor is determined from galvanostatic discharge curves using $C = I/(A \times (dV/dt))$, where I is the discharge current, A is the area of one electrode, and dV/dt is calculated from the slope of the discharge curve. Calculating the slope dV/dt can introduce significant errors, and it is important to calculate the capacitance using the typical operating voltage range. The recommended method to calculate the discharge curve is to use two data points with $dV/dt = (V - {}^1/_2V)/(t_2 - t_1)$ where V is the voltage change.[75] The energy density E and power density P can be calculated with $E = {}^1/_2CV^2$ and $P = E/t$, respectively, where t is the discharge time. The capacitance of the supercapacitors decreased to 82% gradually with the increase of the discharge current density from 0.00125 to 0.0125 mA/cm^2 without showing significant reduction in capacitance, indicating a stable electrochemical behavior. The electrode in 30% KOH solution was tested under 200 repetitive stretching cycles with up to 100% strains as shown in Figure 4c. Strains were induced by a manually operated screw stage as shown in Figure S5. The measured capacitance gradually decreased with increasing cycle numbers, which was attenuated to about 75% of the initial value at the 200th cycle. Such high and stable strechability can be ascribed to the excellent integration between interwoven CNTs and PDMS. In Figure 4d, the cyclic performance showed a stable performance during and after 10 000 galvanostatic charge/discharge cycles at a current density of 2.00 mA/cm^2 with its capacitance maintained after the 10 000 charge/discharge cycles. The all-solid-state supercapacitor was stable with an applied potential ranging from 0.5 to 0.8 V as shown in Figure 4e, showing electrochemical stability of the PVA−KOH gel electrolyte. Although higher operating voltages allow for higher energy densities, the CV curves become less symmetric when the voltage is close to 1 V (electrolyte's electrochemical window is reflected by the voltage range from 0 to ∼1 V for aqueous). The overall performance of the all-solid-state flexible

DOI: 10.1021/acsaem.8b00156
ACS Appl. Energy Mater. XXXX, XXX, XXX−XXX

supercapacitor was presented in the form of Ragone plot in Figure S6. From the Ragone plot, with the increase of the current density from 0.00625 to 0.0125 mA/cm^2, the energy density decreased from 0.0601 to 0.0319 mWh/cm^2, while the power density increased from 0.005 413 to 0.009 275 W/cm^2, which was better than or comparable to the values reported in the literature.[16,70,73,76]

We also tested the electrochemical properties of the all-solid-state supercapacitor under strains as shown in Figures 5. In this test, a diode was connected with a 9 V battery, a 1000 Ω resistor, a switch, a voltmeter, and the flexible supercapacitor. The circuit diagram is shown in Figure S7. When the battery was connected, the voltage across the diode was 1.743 V. Then we measured the voltage when the battery was disconnected with/without paralleling the supercapacitor to test the discharging performance of the CNT−PDMS supercapacitor (Figures S7). First, we measured the diode voltage without paralleling the supercapacitor, where the diode voltage was instantly dropped from 1.743 to 0.051 V (Figure S7a). Then, we connected the supercapacitor in parallel with the diode, which are connected to the battery (Figure S7b). The measured diode voltage fully charged by the battery was 1.743 V. Next, we disconnected the battery from the supercapacitor as shown in Figure S7c, and the measured diode voltage was dropped down to 0.944 V after the supercapacitor was discharged for 3 s. The discharge performance of the supercapacitor is shown in Figure 4f. For comparison, we performed the same measurements with various applied strains (i.e., stretching and bending) to the CNT−PDMS substrate (Figures 5c,d). Under about 50% stretching of the supercapacitor substrate, the diode voltage was dropped from 1.742 to 0.818 V, which was similar to the discharge performance without stretching. The discharge performance with the supercapacitor under substrate bending exhibited a nearly identical discharge rate with the values without bending.

4. CONCLUSIONS

We have demonstrated highly stretchable supercapacitors enabled by a unique fabrication strategy, in which individual carbon nanotubes are partially embedded in PDMS, warranting a high level of integrity of interwoven CNT−PDMS structure. A nanotube architecture/network of any shape (pattern) and dimension can be applied with the same transfer method without disrupting the nanotube alignment. The CNT−PDMS structure was used as the supercapacitor electrode and characterized in an ionic liquid electrolyte as well as with a gel electrolyte. The CNTs exhibited electrochemical stability and repeatability in both the ionic liquid electrolyte and the gel electrolyte at the scan rates from 50 to 1000 mV/s. The fabricated CNT−PDMS structures exhibited high flexibility, stretchability, and stability under stretching up to 200%, bending up to 180°, and twisting up to 180°. The CNT carpet consisting of wavy nanotubes individually entangled with each other (i.e., mechanically cross-linked) retained the entanglement under the lateral expansion of the nanotube network, maintaining their mechanical and electrical integrity. The all-solid-state flexible supercapacitors showed a stable cyclic behavior up to 10 000 cycles of galvanostatic charge/discharge measurement. This demonstration is promising for flexible energy storage devices to be compatible with wearable electronics applications.

ASSOCIATED CONTENT

Supporting Information

The Supporting Information is available free of charge on the ACS Publications website at DOI: 10.1021/acsaem.8b00156.

Details of the fabrication and measurement process, cyclic voltammetry (CV) curves at different scan rates, and Ragone plot of the supercapacitors (PDF)

AUTHOR INFORMATION

Corresponding Author

*E-mail eyang@stevens.edu (E.H.Y.).

ORCID

Eui-Hyeok Yang: 0000-0003-4893-1691

Present Address

J.D. and C.L.: Kazuo Inamori School of Engineering, New York State College of Ceramics, Alfred University, Alfred, NY 14802.

Notes

The authors declare no competing financial interest.

ACKNOWLEDGMENTS

This work has been partially carried out in the Micro Device Laboratory (MDL) at Stevens Institute of Technology funded by US Army under Contract No. W15QKN-05-D-0011. The authors also thank Dr. Kyungnam Kang and Mr. Anthony Palumbo for their assistance in preparing the manuscript.

REFERENCES

(1) Conway, B. E. *Electrochemical Supercapacitors: Scientific Fundamentals and Technological Applications*; Springer Science & Business Media: 2013.

(2) Li, X.; Wei, B. Supercapacitors Based on Nanostructured Carbon. *Nano Energy* **2013**, *2*, 159−173.

(3) Kanninen, P.; Luong, N. D.; Anoshkin, I. V.; Tsapenko, A.; Seppälä, J.; Nasibulin, A. G.; Kallio, T.; et al. Transparent and Flexible High-Performance Supercapacitors Based on Single-Walled Carbon Nanotube Films. *Nanotechnology* **2016**, *27*, 235403.

(4) Rogers, J. A.; Someya, T.; Huang, Y. Materials and Mechanics for Stretchable Electronics. *Science* **2010**, *327*, 1603−1607.

(5) Sekitani, T.; Nakajima, H.; Maeda, H.; Fukushima, T.; Aida, T.; Hata, K.; Someya, T. Stretchable Active-Matrix Organic Light-Emitting Diode Display Using Printable Elastic Conductors. *Nat. Mater.* **2009**, *8*, 494−499.

(6) Lipomi, D. J.; Tee, B. C.-K.; Vosgueritchian, M.; Bao, Z. Stretchable Organic Solar Cells. *Adv. Mater.* **2011**, *23*, 1771−1775.

(7) Xu, S.; Zhang, Y.; Cho, J.; Lee, J.; Huang, X.; Jia, L.; Fan, J. A.; Su, Y.; Su, J.; Zhang, H.; et al. Stretchable Batteries with Self-Similar Serpentine Interconnects and Integrated Wireless Recharging Systems. *Nat. Commun.* **2013**, *4*, 1543.

(8) Ding, J.; Fisher, F. T.; Yang, E. H. Direct Transfer of Corrugated Graphene Sheets as Stretchable Electrodes. *J. Vac. Sci. Technol., B: Nanotechnol. Microelectron.: Mater., Process., Meas., Phenom.* **2016**, *34*, 051205.

(9) Cai, L.; Song, L.; Luan, P.; Zhang, Q.; Zhang, N.; Gao, Q.; Zhao, D.; Zhang, X.; Tu, M.; Yang, F.; et al. Super-Stretchable, Transparent Carbon Nanotube-Based Capacitive Strain Sensors for Human Motion Detection. *Sci. Rep.* **2013**, *3*, 3048.

(10) Chae, S. H.; Lee, Y. H. Carbon Nanotubes and Graphene towards Soft Electronics. *Nano Converg.* **2014**, *1*, 1−26.

(11) Inagaki, M.; Konno, H.; Tanaike, O. Carbon Materials for Electrochemical Capacitors. *J. Power Sources* **2010**, *195*, 7880−7903.

(12) Lu, W.; Dai, L. *Carbon Nanotube Supercapacitors*; INTECH Open Access Publisher: 2010.

(13) Zhang, Z.; Dahal, N.; Xu, K.; Choi, D.; Yang, E. H.; Park, J.-R. Electrochemical Characterization of Tin Quantum Dots Grown on a

Carbon Nanotube Mat as an Anode of Batteries for Medical Applications. *Nanosci. Nanotechnol. Lett.* **2010**, *2*, 86−88.
(14) Niu, Z.; Dong, H.; Zhu, B.; Li, J.; Hng, H. H.; Zhou, W.; Chen, X.; Xie, S. Highly Stretchable, Integrated Supercapacitors Based on Single-Walled Carbon Nanotube Films with Continuous Reticulate Architecture. *Adv. Mater.* **2013**, *25*, 1058−1064.
(15) Jeong, H. T.; Kim, B. C.; Higgins, M. J.; Wallace, G. G. Highly Stretchable Reduced Graphene Oxide (rGO)/single-Walled Carbon Nanotubes (SWNTs) Electrodes for Energy Storage Devices. *Electrochim. Acta* **2015**, *163*, 149−160.
(16) Xu, P.; Gu, T.; Cao, Z.; Wei, B.; Yu, J.; Li, F.; Byun, J.-H.; Lu, W.; Li, Q.; Chou, T.-W. Carbon Nanotube Fiber Based Stretchable Wire-Shaped Supercapacitors. *Adv. Energy Mater.* **2014**, *4*, 1300759.
(17) Fan, Z.; Yan, J.; Wei, T.; Zhi, L.; Ning, G.; Li, T.; Wei, F. Asymmetric Supercapacitors Based on graphene/MnO2 and Activated Carbon Nanofiber Electrodes with High Power and Energy Density. *Adv. Funct. Mater.* **2011**, *21*, 2366−2375.
(18) Wang, G.; Wang, H.; Lu, X.; Ling, Y.; Yu, M.; Zhai, T.; Tong, Y.; Li, Y. Solid-State Supercapacitor Based on Activated Carbon Cloths Exhibits Excellent Rate Capability. *Adv. Mater.* **2014**, *26*, 2676−2682.
(19) Pröbstle, H.; Wiener, M.; Fricke, J. Carbon Aerogels for Electrochemical Double Layer Capacitors. *J. Porous Mater.* **2003**, *10*, 213−222.
(20) Liu, C.; Yu, Z.; Neff, D.; Zhamu, A.; Jang, B. Z. Graphene-Based Supercapacitor with an Ultrahigh Energy Density. *Nano Lett.* **2010**, *10*, 4863−4868.
(21) Ma, Y.; Li, P.; Sedloff, J. W.; Zhang, X.; Zhang, H.; Liu, J. Conductive Graphene Fibers for Wire-Shaped Supercapacitors Strengthened by Unfunctionalized Few-Walled Carbon Nanotubes. *ACS Nano* **2015**, *9*, 1352−1359.
(22) Kim, Y. S.; Kumar, K.; Fisher, F. T.; Yang, E. H. Out-of-Plane Growth of CNTs on Graphene for Supercapacitor Applications. *Nanotechnology* **2012**, *23*, 015301.
(23) Zang, J.; Cao, C.; Feng, Y.; Liu, J.; Zhao, X. Stretchable and High-Performance Supercapacitors with Crumpled Graphene Papers. *Sci. Rep.* **2015**, *4*, 6492.
(24) El-Kady, M. F.; Kaner, R. B. Scalable Fabrication of High-Power Graphene Micro-Supercapacitors for Flexible and on-Chip Energy Storage. *Nat. Commun.* **2013**, *4*, 1475.
(25) Chen, T.; Xue, Y.; Roy, A. K.; Dai, L. Transparent and Stretchable High-Performance Supercapacitors Based on Wrinkled Graphene Electrodes. *ACS Nano* **2014**, *8*, 1039−1046.
(26) Liu, L.; Niu, Z.; Zhang, L.; Zhou, W.; Chen, X.; Xie, S. Nanostructured Graphene Composite Papers for Highly Flexible and Foldable Supercapacitors. *Adv. Mater.* **2014**, *26*, 4855−4862.
(27) Yu, D.; Goh, K.; Wang, H.; Wei, L.; Jiang, W.; Zhang, Q.; Dai, L.; Chen, Y. Scalable Synthesis of Hierarchically Structured Carbon Nanotube-Graphene Fibres for Capacitive Energy Storage. *Nat. Nanotechnol.* **2014**, *9*, 555−562.
(28) Yu, C.; Masarapu, C.; Rong, J.; Wei, B.; Jiang, H. Stretchable Supercapacitors Based on Buckled Single-Walled Carbon-Nanotube Macrofilms. *Adv. Mater.* **2009**, *21*, 4793−4797.
(29) Lee, M.-S.; Lee, K.; Kim, S.-Y.; Lee, H.; Park, J.; Choi, K.-H.; Kim, H.-K.; Kim, D.-G.; Lee, D.-Y.; Nam, S.; et al. High-Performance, Transparent, and Stretchable Electrodes Using Graphene−Metal Nanowire Hybrid Structures. *Nano Lett.* **2013**, *13*, 2814−2821.
(30) Lee, J. A.; Shin, M. K.; Kim, S. H.; Cho, H. U.; Spinks, G. M.; Wallace, G. G.; Lima, M. D.; Lepró, X.; Kozlov, M. E.; Baughman, R. H. Ultrafast Charge and Discharge Biscrolled Yarn Supercapacitors for Textiles and Microdevices. *Nat. Commun.* **2013**, *4*, 1970.
(31) Ren, J.; Li, L.; Chen, C.; Chen, X.; Cai, Z.; Qiu, L.; Wang, Y.; Zhu, X.; Peng, H. Twisting Carbon Nanotube Fibers for Both Wire-Shaped Micro-Supercapacitor and Micro-Battery. *Adv. Mater.* **2013**, *25*, 1155−1159.
(32) Xie, Y.; Liu, Y.; Zhao, Y.; Tsang, Y. H.; Lau, S. P.; Huang, H.; Chai, Y. Stretchable All-Solid-State Supercapacitor with Wavy Shaped Polyaniline/graphene Electrode. *J. Mater. Chem. A* **2014**, *2*, 9142−9149.
(33) Choi, D.; Yang, E. H.; Gill, W.; Berndt, A.; Park, J.-R.; Ryu, J. E. Fabrication and Electrochemical Characterization of Super-Capacitor Based on Three-Dimensional Composite Structure of Graphene and a Vertical Array of Carbon Nanotubes. *J. Compos. Mater.* **2018**.
(34) Frackowiak, E. Carbon Materials for Supercapacitor Application. *Phys. Chem. Chem. Phys.* **2007**, *9*, 1774−1785.
(35) Pan, H.; Li, J.; Feng, Y. Carbon Nanotubes for Supercapacitor. *Nanoscale Res. Lett.* **2010**, *5*, 654.
(36) Frackowiak, E.; Metenier, K.; Bertagna, V.; Beguin, F. Supercapacitor Electrodes from Multiwalled Carbon Nanotubes. *Appl. Phys. Lett.* **2000**, *77*, 2421−2423.
(37) Niu, C.; Sichel, E. K.; Hoch, R.; Moy, D.; Tennent, H. High Power Electrochemical Capacitors Based on Carbon Nanotube Electrodes. *Appl. Phys. Lett.* **1997**, *70*, 1480−1482.
(38) De Volder, M. F. L.; Tawfick, S. H.; Baughman, R. H.; Hart, A. J. Carbon Nanotubes: Present and Future Commercial Applications. *Science (Washington, DC, U. S.)* **2013**, *339*, 535−539.
(39) Yuksel, R.; Sarioba, Z.; Cirpan, A.; Hiralal, P.; Unalan, H. E. Transparent and Flexible Supercapacitors with Single Walled Carbon Nanotube Thin Film Electrodes. *ACS Appl. Mater. Interfaces* **2014**, *6*, 15434−15439.
(40) Huang, K.-J.; Wang, L.; Zhang, J.-Z.; Wang, L.-L.; Mo, Y.-P. One-Step Preparation of Layered Molybdenum Disulfide/multi-Walled Carbon Nanotube Composites for Enhanced Performance Supercapacitor. *Energy* **2014**, *67*, 234−240.
(41) Zhang, H.; Cao, G. P.; Yang, Y. S. Using a Cut−Paste Method to Prepare a Carbon Nanotube Fur Electrode. *Nanotechnology* **2007**, *18*, 195607.
(42) Honda, Y.; Takeshige, M.; Shiozaki, H.; Kitamura, T.; Yoshikawa, K.; Chakrabarti, S.; Suekane, O.; Pan, L.; Nakayama, Y.; Yamagata, M.; et al. Vertically Aligned Double-Walled Carbon Nanotube Electrode Prepared by Transfer Methodology for Electric Double Layer Capacitor. *J. Power Sources* **2008**, *185*, 1580−1584.
(43) Honda, Y.; Haramoto, T.; Takeshige, M.; Shiozaki, H.; Kitamura, T.; Ishikawa, M. Aligned MWCNT Sheet Electrodes Prepared by Transfer Methodology Providing High-Power Capacitor Performance. *Electrochem. Solid-State Lett.* **2007**, *10*, A106−A110.
(44) Kim, B.; Chung, H.; Kim, W. High-Performance Supercapacitors Based on Vertically Aligned Carbon Nanotubes and Nonaqueous Electrolytes. *Nanotechnology* **2012**, *23*, 155401.
(45) Lin, Z.; Li, Z.; Moon, K.; Fang, Y.; Yao, Y.; Li, L.; Wong, C. Robust Vertically Aligned Carbon Nanotube−Carbon Fiber Paper Hybrid as Versatile Electrodes for Supercapacitors and Capacitive Deionization. *Carbon* **2013**, *63*, 547−553.
(46) Park, S.; Vosguerichian, M.; Bao, Z. A Review of Fabrication and Applications of Carbon Nanotube Film-Based Flexible Electronics. *Nanoscale* **2013**, *5*, 1727−1752.
(47) Jiang, Y.; Wang, P.; Zang, X.; Yang, Y.; Kozinda, A.; Lin, L. Uniformly Embedded Metal Oxide Nanoparticles in Vertically Aligned Carbon Nanotube Forests as Pseudocapacitor Electrodes for Enhanced Energy Storage. *Nano Lett.* **2013**, *13*, 3524−3530.
(48) Sun, G.; Zhang, X.; Lin, R.; Yang, J.; Zhang, H.; Chen, P. Hybrid Fibers Made of Molybdenum Disulfide, Reduced Graphene Oxide, and Multi-Walled Carbon Nanotubes for Solid-State, Flexible, Asymmetric Supercapacitors. *Angew. Chem., Int. Ed.* **2015**, *54*, 4651−4656.
(49) Hiraoka, T.; Izadi-Najafabadi, A.; Yamada, T.; Futaba, D. N.; Yasuda, S.; Tanaike, O.; Hatori, H.; Yumura, M.; Iijima, S.; Hata, K. Compact and Light Supercapacitor Electrodes from a Surface-Only Solid by Opened Carbon Nanotubes with 2 200 m2 G- 1 Surface Area. *Adv. Funct. Mater.* **2010**, *20*, 422−428.
(50) Jakubinek, M. B.; White, M. A.; Li, G.; Jayasinghe, C.; Cho, W.; Schulz, M. J.; Shanov, V. Thermal and Electrical Conductivity of Tall, Vertically Aligned Carbon Nanotube Arrays. *Carbon* **2010**, *48*, 3947−3952.
(51) Chen, T.; Peng, H.; Durstock, M.; Dai, L. High-Performance Transparent and Stretchable All-Solid Supercapacitors Based on Highly Aligned Carbon Nanotube Sheets. *Sci. Rep.* **2015**, *4*, 3612.
(52) Hsia, B.; Marschewski, J.; Wang, S.; In, J. B.; Carraro, C.; Poulikakos, D.; Grigoropoulos, C. P.; Maboudian, R. Highly Flexible,

DOI: 10.1021/acsaem.8b00156
ACS Appl. Energy Mater. XXXX, XXX, XXX−XXX

All Solid-State Micro-Supercapacitors from Vertically Aligned Carbon Nanotubes. *Nanotechnology* **2014**, *25*, 055401.
(53) Zeng, S.; Chen, H.; Cai, F.; Kang, Y.; Chen, M.; Li, Q. Electrochemical Fabrication of Carbon Nanotube/polyaniline Hydrogel Film for All-Solid-State Flexible Supercapacitor with High Areal Capacitance. *J. Mater. Chem. A* **2015**, *3*, 23864−23870.
(54) Zhang, Z.; Xiao, F.; Qian, L.; Xiao, J.; Wang, S.; Liu, Y. Facile Synthesis of 3D MnO_2–Graphene and Carbon Nanotube–Graphene Composite Networks for High-Performance, Flexible, All-Solid-State Asymmetric Supercapacitors. *Adv. Energy Mater.* **2014**, *4*, 1400064.
(55) Zhang, Z.; Deng, J.; Li, X.; Yang, Z.; He, S.; Chen, X.; Guan, G.; Ren, J.; Peng, H. Superelastic Supercapacitors with High Performances during Stretching. *Adv. Mater.* **2015**, *27*, 356−362.
(56) Qiu, Y.; Li, G.; Hou, Y.; Pan, Z.; Li, H.; Li, W.; Liu, M.; Ye, F.; Yang, X.; Zhang, Y. Vertically Aligned Carbon Nanotubes on Carbon Nanofibers: A Hierarchical Three-Dimensional Carbon Nanostructure for High-Energy Flexible Supercapacitors. *Chem. Mater.* **2015**, *27*, 1194−1200.
(57) Jung, Y. J.; Kar, S.; Talapatra, S.; Soldano, C.; Viswanathan, G.; Li, X.; Yao, Z.; Ou, F. S.; Avadhanula, A.; Vajtai, R.; et al. Aligned Carbon Nanotube- Polymer Hybrid Architectures for Diverse Flexible Electronic Applications. *Nano Lett.* **2006**, *6*, 413−418.
(58) Choi, C.; Lee, J. A.; Choi, A. Y.; Kim, Y. T.; Lepró, X.; Lima, M. D.; Baughman, R. H.; Kim, S. J. Flexible Supercapacitor Made of Carbon Nanotube Yarn with Internal Pores. *Adv. Mater.* **2014**, *26*, 2059−2065.
(59) Liu, J.; Zhang, L.; Wu, H. B.; Lin, J.; Shen, Z.; Lou, X. W. D. High-Performance Flexible Asymmetric Supercapacitors Based on a New Graphene Foam/carbon Nanotube Hybrid Film. *Energy Environ. Sci.* **2014**, *7*, 3709−3719.
(60) Fu, Y.; Cai, X.; Wu, H.; Lv, Z.; Hou, S.; Peng, M.; Yu, X.; Zou, D. Fiber Supercapacitors Utilizing Pen Ink for Flexible/wearable Energy Storage. *Adv. Mater.* **2012**, *24*, 5713−5718.
(61) Kumar, K.; Kim, Y. S.; Li, X.; Ding, J.; Fisher, F. T.; Yang, E. H. Chemical Vapor Deposition of Carbon Nanotubes on Monolayer Graphene Substrates: Reduced Etching via Suppressed Catalytic Hydrogenation Using C2H4. *Chem. Mater.* **2013**, *25*, 3874−3879.
(62) Ding, J.; Fu, S.; Zhang, R.; Boon, E.; Lee, W.; Fisher, F.; Yang, E. H. Graphene−Vertically Aligned Carbon Nanotube Hybrid on PDMS as Stretchable Electrodes. *Nanotechnology* **2017**, *28*, 465302.
(63) Qiu, W.; Li, Q.; Lei, Z.-K.; Qin, Q.-H.; Deng, W.-L.; Kang, Y.-L. The Use of a Carbon Nanotube Sensor for Measuring Strain by Micro-Raman Spectroscopy. *Carbon* **2013**, *53*, 161−168.
(64) Chang, C.-C.; Chen, C.-C.; Hung, W.-H.; Hsu, I.-K.; Pimenta, M. A.; Cronin, S. B. Strain-Induced D Band Observed in Carbon Nanotubes. *Nano Res.* **2012**, *5*, 854−862.
(65) Cooper, C. A.; Young, R. J.; Halsall, M. Investigation into the Deformation of Carbon Nanotubes and Their Composites through the Use of Raman Spectroscopy. *Composites, Part A* **2001**, *32*, 401−411.
(66) Duan, X.; Son, H.; Gao, B.; Zhang, J.; Wu, T.; Samsonidze, G. G.; Dresselhaus, M. S.; Liu, Z.; Kong, J. Resonant Raman Spectroscopy of Individual Strained Single-Wall Carbon Nanotubes. *Nano Lett.* **2007**, *7*, 2116−2121.
(67) Wei, Q.; Yi-Lan, K.; Zhen-Kun, L.; Qing-Hua, Q.; Qiu, L. A New Theoretical Model of a Carbon Nanotube Strain Sensor. *Chin. Phys. Lett.* **2009**, *26*, 080701.
(68) Wang, W.; Guo, S.; Penchev, M.; Ruiz, I.; Bozhilov, K. N.; Yan, D.; Ozkan, M.; Ozkan, C. S. Three Dimensional Few Layer Graphene and Carbon Nanotube Foam Architectures for High Fidelity Supercapacitors. *Nano Energy* **2013**, *2*, 294−303.
(69) Bae, J.; Park, Y. J.; Lee, M.; Cha, S. N.; Choi, Y. J.; Lee, C. S.; Kim, J. M.; Wang, Z. L. Single-Fiber-Based Hybridization of Energy Converters and Storage Units Using Graphene as Electrodes. *Adv. Mater.* **2011**, *23*, 3446−3449.
(70) Bae, J.; Song, M. K.; Park, Y. J.; Kim, J. M.; Liu, M.; Wang, Z. L. Fiber Supercapacitors Made of Nanowire-Fiber Hybrid Structures for Wearable/Flexible Energy Storage. *Angew. Chem., Int. Ed.* **2011**, *50*, 1683−1687.
(71) Kaempgen, M.; Chan, C. K.; Ma, J.; Cui, Y.; Gruner, G. Printable Thin Film Supercapacitors Using Single-Walled Carbon Nanotubes. *Nano Lett.* **2009**, *9*, 1872−1876.
(72) In, H. J.; Kumar, S.; Shao-Horn, Y.; Barbastathis, G. Origami Fabrication of Nanostructured, Three-Dimensional Devices: Electrochemical Capacitors with Carbon Electrodes. *Appl. Phys. Lett.* **2006**, *88*, 083104.
(73) Meng, Y.; Zhao, Y.; Hu, C.; Cheng, H.; Hu, Y.; Zhang, Z.; Shi, G.; Qu, L. All-Graphene Core-Sheath Microfibers for All-Solid-State, Stretchable Fibriform Supercapacitors and Wearable Electronic Textiles. *Adv. Mater.* **2013**, *25*, 2326−2331.
(74) Gao, K.; Shao, Z.; Wu, X.; Wang, X.; Zhang, Y.; Wang, W.; Wang, F. Based Transparent Flexible Thin Film Supercapacitors. *Nanoscale* **2013**, *5*, 5307−5311.
(75) Stoller, M. D.; Ruoff, R. S. Best Practice Methods for Determining an Electrode Material's Performance for Ultracapacitors. *Energy Environ. Sci.* **2010**, *3*, 1294−1301.
(76) Gao, Y.; Zhou, Y. S.; Xiong, W.; Jiang, L. J.; Mahjouri-Samani, M.; Thirugnanam, P.; Huang, X.; Wang, M. M.; Jiang, L.; Lu, Y. F. Transparent, Flexible, and Solid-State Supercapacitors Based on Graphene Electrodes. *APL Mater.* **2013**, *1*, 012101.

DOI: 10.1021/acsaem.8b00156
ACS Appl. Energy Mater. XXXX, XXX, XXX−XXX